

## A tale of two cities

### Vulnerabilities of the London and Paris transit networks

Christian von Ferber · Bertrand Berche ·  
Taras Holovatch · Yurij Holovatch

Received: date / Accepted: date

**Abstract** This paper analyses the impact of random failure or attack on the public transit networks of London and Paris in a comparative study. In particular we analyze how the dysfunction or removal of sets of stations or links (rails, roads, etc.) affects the connectivity properties within these networks. We show how accumulating dysfunction leads to emergent phenomena that cause the transportation system to break down as a whole. Simulating different directed attack strategies, we find minimal strategies with high impact and identify a-priori criteria that correlate with the resilience of these networks. To demonstrate our approach, we choose the London and Paris public transit networks. Our quantitative analysis is performed in the frames of the complex network theory – a methodological tool that has emerged recently as an interdisciplinary approach joining methods and concepts of the theory of random graphs, percolation, and statistical physics. In conclusion we demonstrate that taking into account cascading effects the network integrity is controlled for both networks by less than 0.5% of the stations i.e. 19 for Paris and 34 for London.

**Keywords** public transit · attack vulnerability · complex networks · percolation

**PACS** 02.50.-r · 07.05.Rm · 89.75.Hc

**Mathematics Subject Classification (2000)** 05C82 · 82B43 · 94C15

---

Christian von Ferber  
Applied Math. Research Centre, Coventry University, UK

Bertrand Berche  
Institut Jean Lamour, Université de Lorraine, Vandœuvre les Nancy, France

Taras Holovatch  
Applied Math. Research Centre, Coventry University, UK & Institut Jean Lamour, Université de Lorraine, Vandœuvre les Nancy, France

Yurij Holovatch  
Institute for Condensed Matter Physics, National Acad. Sci. of Ukraine, Lviv, Ukraine

## 1 Introduction

"The traveller fared slowly on his way, who fared towards Paris from England in the autumn of the year one thousand seven hundred and ninety-two. More than enough of bad roads, bad equipages, and bad horses, he would have encountered to delay him".<sup>1</sup> In the times when Charles Dickens wrote these words in his famous novel, there was perhaps not too much difference concerning the quality of transportation systems in the two cities, or reasons that may have caused their malfunction. Historical circumstances may have had a different impact on the development of public transit security in both cities. However, today one might assume that on average the differences observed between the facilities offered by transportation networks of developed countries may be small enough. Analyzing the readily available data on these networks both with algorithms and analytical approaches we test this assumption and quantify remaining differences.

The aim of this paper is to compare security features of highly developed contemporary public transit networks (PTN) - of two European capitals, London and Paris. These cities were chosen as they display similarities in their structure and historical development caused by geographical and social reasons and further due to the particular role of the public transit facilities of London in the wake of the 2012 Olympics. We will be interested in the impact of both random failure and targeted attacks that may lead to dysfunction either within the stations of the PTN or along the links (rails, roads, bridges, etc.) that connect them. In a general approach to this problem one would want to consider a dynamic model of the PTN including the current local capacities and loads at the time of failure, detailed passenger destinations and itinerary together with a full view of the PTN structure (i.e. topological and connectivity properties of the network). In lack of availability of corresponding data for such an approach we restrict our study to the impact of failure on the topological and connectivity properties of the analyzed networks. This provides a first but essential step towards understanding how vulnerabilities may be reduced by choosing appropriate network topologies. In particular, we will consider the static network structure of the PTNs of London and Paris and analyze their vulnerability with respect to dysfunction due to random failure or directed attack. As we will see below, simulating various failure and attack scenarios even on this level illuminates significant differences and allows for general conclusions concerning the behavior of these PTNs under stress.

The setup of this paper is as follows. In the next section we briefly describe the general method of our analysis – complex network theory [1,2] – and present an overview on previous studies. We proceed to discuss the problem of PTN vulnerability in section 3, where we show how this problem is related to the percolation theory [3]. We introduce observables that quantitatively measure the impact on PTNs under attack, a problem we further analyze in section 4 where we present a comparative analysis of the London and Paris

---

<sup>1</sup> Charles Dickens. *A Tale of Two Cities*. London: Penguin Classics (2003).

PTNs and the impact of failure and attacks of different nature. We discuss possible reasons for the differences observed for PTN vulnerability and propose estimators for local and global properties that allow a priori assessment of the degree of resilience or vulnerability of PTNs. Taking into account cascading effects in the interplay between routes and stations we demonstrate in section 5 that the network integrity hinges on the effective operation of a very small set of important stations.

## 2 A complex network model of public transit

The observation that the paths of public transit routes of a city form a network and that this network is complex enough is part of our everyday experience. However, the concept of *complex networks* has recently become the nucleus of a new and rapidly developing field of knowledge that has its roots in random graph theory and statistical physics (see e.g. recent reviews [1] and monographs [2]). From a mathematical point of view, a network is nothing else but a graph defined by a set of vertexes and a set of edges or links each connecting a pair of vertexes. Graph theory is well-settled branch of discrete mathematics with origins in classical works of L. Euler [4]. An essential breakthrough and a paradigm shift in graph theory (and in particular concerning random graphs) occurred in the 1990-ies, when particular correlations were discovered in otherwise seemingly random graphs. It was realized, that numerous natural and man-made structures may be described in terms of networks and that these networks possess surprising properties, strikingly different from those of the so-called classical random graph [5]. Such networks are currently classified as complex networks. To name a few, these include networks describing interacting systems of biological, ecological, sociological or technological origins such as networks of cell metabolism, communication, transportation, and many other forms of interaction. Complex networks have been found to be compact structures (sometimes called *small worlds*) with short distances between nodes, and a high level of correlation and self-organization. They demonstrate extremely high resilience with respect to random failure. However they are proven to be particularly vulnerable with respect to targeted attacks. Some of their statistical properties, in particular the distribution of node degrees (the number of connections of individual nodes) are governed by power laws. This indicates the presence of non-trivial correlations within the structure of these systems. We set out to show that similar properties are inherent to the PTN of London and Paris studied in the present work.

Recent research [6, 7, 8, 9, 10, 11, 12] on public transit networks has produced quantitative evidence that PTNs share general features of other transportation or transmission networks like airport, railway, or power grid networks [1]. These features include evolutionary growth, optimization, and usually an embedding in two dimensional (2D) space. Earlier empirical studies of PTNs in the frames of complex network theory have often restricted the analysis to certain sub-networks of city transit. Examples are studies of subway networks of Boston

**Table 1** Characteristics of the PTNs analyzed in this study.  $N$ : number of stations;  $R$ : number of routes. Given characteristics are:  $\langle k \rangle$  (mean node degree);  $\ell^{\max}$ ,  $\langle \ell \rangle$  (maximal and mean shortest path length);  $\mathcal{C}$  (relation of the mean clustering coefficient to that of the classical random graph of equal size, (3) );  $\mathcal{C}_B$ : betweenness centrality (5);  $\kappa^{(z)}$ ,  $\kappa^{(k)}$  (c.f. Eqs. (11), (9)); degree distribution exponent  $\gamma$  (4). Additional details may be found in [11].

City	$N$	$R$	$\langle k \rangle$	$\ell^{\max}$	$\langle \ell \rangle$	$\mathcal{C}$	$\mathcal{C}_B$	$\kappa^{(z)}$	$\kappa^{(k)}$	$\gamma$
London	10937	922	2.60	107	26.5	320.6	$1.4 \cdot 10^5$	1.87	3.22	4.48
Paris	3728	251	3.73	28	6.4	78.5	$1.0 \cdot 10^4$	5.32	6.93	2.62

[6, 7], Vienna [7] and several other cities [8], and city bus networks in Poland [9] and China [10]. However, as far as the bus-, subway- or tram-subnetworks are not closed systems the inclusion of additional subnetworks has significant impact on the overall network properties as has been shown for the subway and bus networks of Boston [6]. Therefore, further analysis of PTN has included the full set of subnetworks [11].

The two PTNs analyzed within the present work are either operated by a single operator (Traffic for London, TFL) or by small number of operators with a coordinated schedule (three operators for Paris), as expressed by a central web site from which our data was obtained.<sup>2</sup> The analyzed PTN of London covers the metropolitan area of 'Greater London' and includes buses, subway, and tram. Correspondingly, the PTN of Paris as analyzed here covers the metropolitan area 'aire urbaine' and comprises buses, RER and subway. Some characteristics of these networks are given in Table 1. There is a number of different ways to represent a PTN in the form of a graph [6, 7, 8, 9, 10, 11, 12, 13]. In what follows below, we will mostly use the so-called **L**-space representation [6, 9, 11], where each public transit station is represented by a vertex (node) and any two stations serviced successively by at least one route are connected by an edge (link). In this representation the obtained graph – a complex network – is most similar to the PTN map.<sup>3</sup> Typical measures for the 'diameter' of the network are the maximal or the mean *shortest path* lengths  $\ell^{\max}$  and  $\langle \ell \rangle$ . The latter is defined by:

$$\langle \ell \rangle = \frac{2}{N(N-1)} \sum_{i>j \in \mathcal{N}} \ell(i, j), \quad (1)$$

where  $N$  is the number of network nodes,  $\ell(i, j)$  is the length of a shortest path (in terms of station intervals traveled) between nodes  $i$  and  $j$  and the sum spans all pairs  $i, j$  of sites that belong to the network  $\mathcal{N}$ . The comparatively low values of  $\langle \ell \rangle$  found for the two PTNs (see Table 1) may be related to their small world structure (where  $\langle \ell \rangle$  shows logarithmic growth with the number of nodes) [11]. The fact that the London PTN has a larger value  $\ell^{\max}$  corresponds to the larger area covered by the network (as seen, e.g. from larger number of routes and stations).

<sup>2</sup> See [11] for more details on the database.

<sup>3</sup> Note, however that multiple links are absent in this graph.

The mean and maximal shortest path lengths characterize the network as a whole and sometimes are referred to as global properties of the network. An example of a local property is given by the node degree  $k_i$ , the number of links that are connected to the node  $i$ . By definition, it is equal to the number of nodes adjacent to the given one and defines the neighborhood size of this node. Obviously, not all neighbors of the node  $i$  need to be neighbors of each other. This property is measured by the *clustering coefficient*:

$$C_i = \frac{2y_i}{k_i(k_i - 1)}, \quad k_i \geq 2, \quad (2)$$

where  $y_i$  is the number of links between the neighbors of node  $i$  and  $C_i = 0$  for  $k_i = 0, 1$ . In general, clustering reflects a specific form of correlation present in a network: the clustering coefficient of a node may also be interpreted as the probability of any two of its neighbors to be connected. A useful numerical indicator is given by the ratio of the mean clustering coefficient of a network to the corresponding value for the classical Erdős-Rényi random graph of equal size:

$$\mathcal{C} = \langle C_i \rangle / C_{ER}. \quad (3)$$

Here,  $C_{ER} = 2M/N^2$  where the classical Erdős-Rényi random graph is constructed by randomly linking  $N$  nodes by  $M$  links [1,2]. Therefore, the high values of  $\mathcal{C}$  found in Table 1 for London and Paris indicate strong local correlations in these networks. Moreover, the London PTN appears locally to be stronger correlated than that of Paris.

Another striking difference between the properties of random graphs and the PTNs considered here is the behavior of the *node-degree distribution*  $P(k)$ , the probability that an arbitrary node is of degree  $k$ . The random graph is characterized by a Poisson distribution which decays exponentially for large  $k$  [1,2]. The empirically observed distributions for the London and Paris PTNs however show a decay best described by a power law [11] :

$$P(k) \sim k^{-\gamma}, \quad k \gg 1. \quad (4)$$

The power law decay (4) indicates *scale-free* properties of the London and Paris PTNs. It is instructive to note that the exponent  $\gamma$  governing this decay is much smaller for the PTN of Paris, see Table 1. As we will show this has important impact on the observed resilience of the network.

To some extent, the node degree may be considered as a local measure of the importance of the node: it is intuitively reasonable that hubs (nodes with a high degree) play an essential role in networks. The importance of a node with respect to the connectivity between other nodes of the network, however, is more efficiently measured by the so-called *betweenness centrality*. For a given node  $i$ , the latter measures the overall share of shortest paths between pairs of other nodes that pass through this node. The betweenness of node  $i$  may be calculated as:

$$C_B(i) = \sum_{j \neq i \neq k \in \mathcal{N}} \frac{\sigma_{jk}(i)}{\sigma_{jk}} \quad (5)$$

where  $\sigma_{jk}$  is the number of shortest paths between nodes  $j$  and  $k$  of the network  $\mathcal{N}$  and  $\sigma_{jk}(i)$  is the number of these paths that go via node  $i$ . Numerical values of the mean betweenness are given in Table 1 for both PTNs.

### 3 PTN resilience: observables and attack scenarios

The impact on complex network behavior upon removal of either their nodes or links is closely related to so-called lattice percolation phenomena [3]. The latter occurs on homogeneous structures (lattices) whereas the non-homogeneity of complex networks gives rise to a variety of phenomena specific for these structures. The empirical analysis of scale-free real-world networks has shown that these networks display unexpectedly high degrees of robustness under random failure [1,2]. However they may be particularly vulnerable to attacks, that target important nodes or links. As we have seen in the previous section, both the London and the Paris PTN share common features of complex networks. Therefore, we may expect their behavior under stress or attack to be similar.

The first property a transit network trivially needs to fulfil is overall connectivity: there must be a path within the network between any two nodes. Upon failure of a smaller or larger set of nodes this overall connectivity may get lost. Generally one considers a network to remain functional if a significantly large connected component (sometimes called a spanning cluster) remains connected.

The phenomenon of the appearance and nature of such spanning clusters is at the center of a well established field of Statistical Physics: *percolation theory* [3]. Originally it describes the emergence of such spanning clusters on a lattice at a certain threshold for the concentration  $c_{\text{perc}}$  of links or nodes present on the lattice and predicts universal properties that may be observed and calculated within the theory with high precision.

On a lattice, the appearance of a spanning cluster signals the onset of percolation at a particular concentration  $c_{\text{perc}}$  of lattice occupation. In turn, the probability that an arbitrary chosen lattice site belongs to the spanning cluster is naturally used as an order parameter: it is equal one for  $c = 1$ , zero for  $c < c_{\text{perc}}$  and follows universal behavior as  $c$  approaches  $c_{\text{perc}}$  from above. A similar percolation phenomenon occurs when a *giant connected component* emerges on an idealized complex network. The giant connected component is understood as a connected subnetwork which in the limit of an infinite network contains a finite fraction of the network. As far as real world networks are finite, the giant component is not well defined. Instead we will observe the size  $N_1(c)$  of the largest connected component in the network to monitor the behavior of the network as function of the share  $c$  of nodes or links that are removed in sequence. For convenience we define the relative size (or share) of the largest component as the ratio of  $N_1(c)$  to  $N$ , the number of nodes in the initial unperturbed network:

$$S(c) = N_1(c)/N. \quad (6)$$

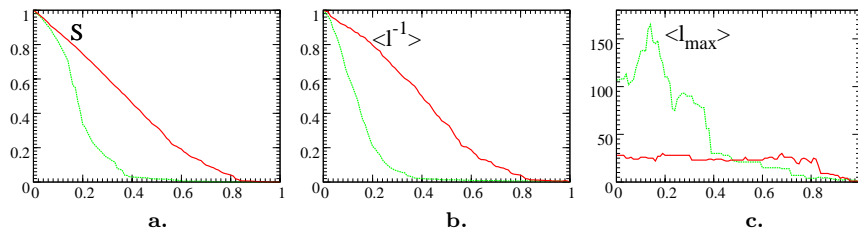


**Fig. 1** Share of the largest component  $S$  (a), mean inverse  $\langle \ell^{-1} \rangle$  (b) and maximal  $\ell^{\max}$  (c) shortest path length as function of the removed share  $c$  of nodes for the PTN of London (light green curve) and Paris (dark red curve). Random removal of PTN nodes.

Another variable that may be used to monitor changes in network structure as nodes or links are removed is the mean inverse shortest path length [14]:

$$\langle \ell^{-1} \rangle = \frac{2}{N(N-1)} \sum_{i>j \in \mathcal{N}} \ell^{-1}(i, j). \quad (7)$$

Here, as in (1),  $\ell(i, j)$  is the shortest path between nodes  $i$  and  $j$  that belong to the network  $\mathcal{N}$ . Note however, that while (1) is ill-defined for the disconnected network, the quantity (7) is well-defined as far as  $\ell^{-1}(i, j) = 0$  if nodes  $i, j$  are disconnected. It may therefore be used to trace impact on the network under attack.

In Figs. 1 a, b we show the behavior of  $S$  and  $\langle \ell^{-1} \rangle$  for the PTN of London and Paris as function of the share of removed nodes  $c$ , as these are removed at random. Already this simple random approach to probe the PTN behavior under attack shows a higher vulnerability of the London PTN to random removal of its nodes: both the  $S$ - and  $\langle \ell^{-1} \rangle$ -curves indicate a faster decay in the case of London PTN. Moreover, the  $S$ -curve for the Paris PTN decays almost linearly. This indicates that sub-clusters less connected to the overall network are almost absent. The size of the largest component decreases only due to the removed nodes. This observation will be further quantified in the next section. Here, we want to support it by displaying the maximal shortest path length behavior, Fig. 1 c. As a matter of fact,  $\ell^{\max}$  manifests very different behavior for these two PTN. For the London PTN,  $\ell^{\max}$  grows initially and then, when a certain threshold is reached ( $c \sim 0.14$ ) it abruptly decreases. Obviously, removing the nodes initially increases the path lengths as deviations from the original shortest paths need to be taken into account. At some point, removing further nodes then leads to a breakup of the network into smaller components on which the paths are naturally limited which explains the sudden decrease of their lengths. Such peculiarities in the behavior of  $\ell^{\max}$  are almost absent for the Paris PTN, at least for small and medium values of  $c$ .

Note, that the plots of Fig. 1 display the results of a single random sequence of node removal. However, as we have checked statistics over large number of random attack sequences [13,15], the large PTN size leads to a 'self-averaging' effect: averaging over many random attack sequences gives results almost identical to those presented in Fig. 1. To further analyze the PTN

attack vulnerability, we have made a series of computer simulations removing PTN nodes and links not at random, but ordering them according to their importance with respect to network connectivity, scenarios we call *attack* or *directed attack*. To order these we use the already mentioned properties such as node degree, betweenness centrality (5), clustering coefficient (2) and several other indicators (see [13,15]). Another attack scenario that has proven successful in immunization problems on complex networks [17] consists in removing of a randomly chosen neighbor of a randomly chosen node. Its efficiency is based on the fact, that in this way nodes with a high number of neighbors will be selected with higher probability. Each of the above described scenarios (except for the random ones) was realized for the lists prepared for the initial network or lists rebuilt by recalculating the order of the remaining nodes after each step. The latter way is known to be usually more efficient and leads to slightly different results suggesting that the network structure changes in the course of the attack [14,18].

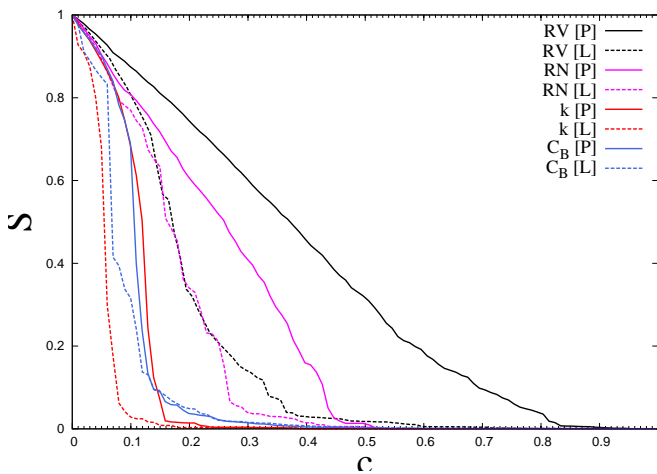


**Fig. 2** Relative size  $S$  of the largest component of the London and Paris PTNs as function of the share  $c$  of removed nodes either chosen at random, or ordered by decreasing node degree  $k$  or betweenness  $C_B$  centrality. The lists were rebuilt by recalculating the order of the remaining nodes after each step. RV (RN): random removal of a node (or of its randomly chosen neighbor). A letter in square brackets refers to the London [L] or Paris [P] PTN.

In Fig. 2 we show the relative size of the largest component of London and Paris PTN as function of the share of nodes removed following specific attack scenarios described above. More specifically, nodes were removed in chunks of 1 % of the initial nodes and a recalculation took place after the removal of each 1% chunk of nodes. As may be drawn from a first glance of the plots, the most harmful are attacks targeted on the nodes of highest node degree and highest betweenness. We will discuss these in more detail in the next section,

complementing the picture of node-targeted attacks by that of attacks that target PTN links.

#### 4 PTN vulnerability: quantitative analysis

In what follows we discuss in some detail those attacks that have highest impact on the two PTNs and compare these with the random attack scenario. To this end, we introduce indicators that quantify PTN resilience [19,20]. Furthermore, we seek correlations between PTN resilience and network characteristics that may be measured independently. We apply this scheme to both node-targeted attacks (section 4.1) and link-targeted attacks (section 4.2).

##### 4.1 Node-targeted attacks

As clearly seen from Figs. 2, if nodes are removed ordered by decreasing degree or betweenness centrality the size  $S$  of the largest component decreases fast and  $S$  is near zero at a share of removed nodes  $c \sim 0.2 \div 0.3$ . In Fig. 3 we further detail this picture giving plots for the size of the largest component  $S$ , mean inverse  $\langle \ell^{-1} \rangle$  and maximal  $\ell^{\max}$  shortest path lengths as function of the removed node share  $c$  for the highest node degree (figures **a** – **c**) and the highest betweenness centrality (figures **d** – **f**) scenarios. Let us compare these with the corresponding plots of Fig. 1, where the impact of random node removal is shown. We observe that for these directed attack scenarios the behavior of both PTNs is not as different as it was observed for the random scenario. Although for the highest node degree scenario both  $S(c)$  and  $\langle \ell^{-1}(c) \rangle$  curves manifest a faster decay for the London PTN (see Figs. 3 **a**, **b**), the difference is less pronounced in the case of the highest betweenness centrality scenario (Figs. 3 **d**, **e**). The similarity in the performance of both PTNs with respect to such attacks is also obvious in the behavior of the maximal shortest path length  $\ell^{\max}$ . For both London and Paris PTNs one observes a pronounced peak in  $\ell^{\max}(c)$  at  $c \sim 0.06$  and  $c \sim 0.1$  with further, smaller peaks occurring with irregular periodicity indicating the existence of sub-clusters within both networks.

The above comparison of the PTN attack vulnerability is as it stands mostly qualitative. To proceed further with a quantitative analysis, a numerical measure of resilience needs to be defined. In percolation theory, where a spanning cluster occurs abruptly at a given percolation concentration  $c_{\text{perc}}$ , the latter may be used as such a measure. In the case of real-world networks of finite size one rather observes a region of concentrations where the emergent behavior of fast decay occurs. In some studies a characteristic concentration value based on particular behavior of either  $S$ ,  $\langle \ell \rangle$ ,  $\langle \ell^{-1} \rangle$  or  $\ell^{\max}$  has been used to identify network breakdown [14,15]. Here, we focus on the behavior of the largest component of the PTN and follow Ref. [19] to introduce a measure that integrates the network reaction over the whole attack sequence. If  $S(c)$  is

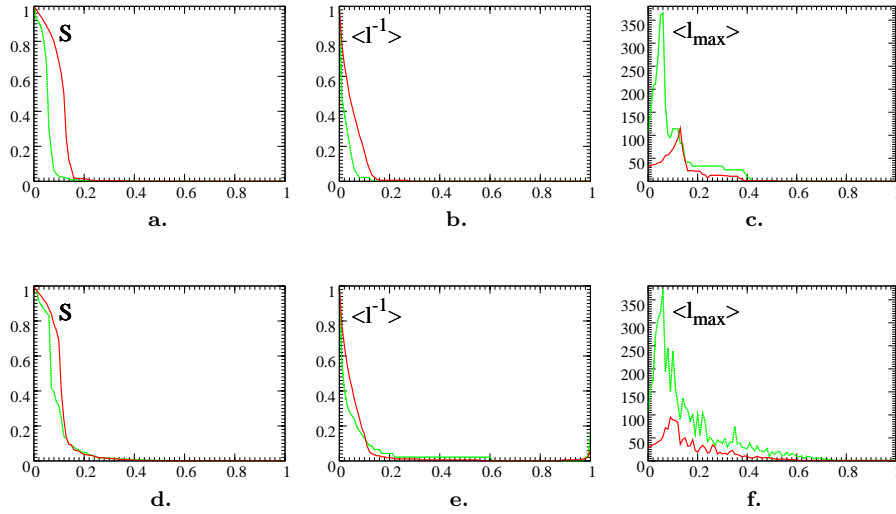


**Fig. 3** Share of the largest component  $S$ , mean inverse  $\langle \ell^{-1} \rangle$  and maximal  $\ell^{\max}$  shortest path length as function of the removed nodes share  $c$  for PTN of London (light green curve) and Paris (dark red curve). **a, b, c**: highest node degree scenario. **d, e, f**: highest betweenness centrality scenario.

the normalized size of the largest component as function of concentration  $c$ , we calculate the area  $A$  below the  $S(c)$  curve as:

$$A = 100 \int_0^1 S(c) dc, \quad (8)$$

and use this as a measure of network resilience. As follows from the definition (8), the measure captures the effects on the network over the complete attack sequence and it is a characteristic measure, well-defined for finite-size networks. The larger the measure  $A$ , the more resilient is the network.

In the left part of table 2 we give the resilience  $A$  for the highest node degree and highest betweenness scenarios and compare with the random scenario. As follows from the table, in almost all instances the Paris PTN shows higher resilience  $A$  than the London PTN. Another conclusion concerns the difference between the value of  $A$  for the random attack (RV) and for attacks that target specific important nodes (with high degree  $k$  or high betweenness centrality  $\mathcal{C}_B$ ): as often observed for complex networks, they are robust with respect to random removal of nodes or links but especially vulnerable to targeted attacks. Naturally the question arises whether such result may be anticipated a priori: can one derive some criteria for PTN resilience prior to the attack? Indeed, the data of Table 1 where information about initial PTN characteristics is summarized allows to at least qualitatively prognosticate the outcome of attacks as summarized in Table 2. For an explanation, let us shortly recall several facts drawn from complex network theory.

For uncorrelated infinite random networks it has been shown [21,22], that a giant connected component is present if the following ratio of moments of

**Table 2** Resilience measure  $A$ , (8), for the PTNs of London and Paris. Columns 2-4 give the value of  $A$  for node-targeted attacks, columns 5-7 give  $A$  for link-targeted attacks. See the text for attack scenario descriptions.

City	Node-targeted attacks			Link-targeted attacks		
	RV	$k$	$C_B$	RL	$k^{(l)}$	$C_B^{(l)}$
London	29.31	5.45	8.71	27.45	20.95	27.2
Paris	37.93	10.77	10.67	56.04	47.12	55.93

the degree distribution

$$\kappa^{(k)} = \langle k^2 \rangle / \langle k \rangle, \quad (9)$$

is greater than two,

$$\kappa^{(k)} \geq 2. \quad (10)$$

Relation (10) is often referred to as the Molloy-Reed criterion and  $\kappa^{(k)}$  is called the Molloy-Reed parameter.

It has been illustrated for many real-world PTN [13,15,20], that the value of the Molloy-Reed parameter for the unperturbed network may be used to estimate network resilience against attack. Typically, networks with low  $\kappa^{(k)}$  appear to be more vulnerable to both random and node degree-targeted attacks. This observation is further supported by monitoring other related parameters, such as the ratio of the mean number  $z_2$  of second neighbors to the mean number  $z_1$  of neighbors:<sup>4</sup>

$$\kappa^{(z)} = z_2 / z_1. \quad (11)$$

It is easy to show that  $\kappa^{(k)} = \kappa^{(z)} + 1$  for uncorrelated networks. As we have seen from the analysis of section 2, strong correlations are present in the PTN and one may not expect a simple relation between parameters  $\kappa^{(k)}$  and  $\kappa^{(z)}$  to hold. However, a comparison of  $\kappa^{(z)}$  for two given networks will provide additional information about their relative resilience.

We have calculated values of  $\kappa^{(k)}$  and  $\kappa^{(z)}$  for the London and Paris PTNs and give them in the ninth and tenth columns of table 1. The corresponding values for the Paris PTN exceed those for London by a factor of two giving a clear signal for a higher vulnerability of the London PTN to random failure. This conclusion has been empirically demonstrated in our simulations reported above.

The higher potential for resilient behavior of the Paris PTN with respect to that of London may also be related to its node-degree distribution. In the last column of table 1 we list the exponent  $\gamma$ , that controls the decay of this distribution. The smaller value of  $\gamma$  for Paris PTN corresponds to the fat-tailed node-degree distribution  $P(k)$ . For an infinite network, the giant connected component is always present for the random attack scenario as long as  $\gamma < 3$  [22] and a smaller values of  $\gamma$  indicate higher network resilience.

<sup>4</sup> By definition  $z_1$  is equal to the mean node degree  $\langle k \rangle$ .

Our analysis has so far described attacks on the network nodes. Before passing to general conclusions, let us further analyze the impact of link-targeted attacks on the two PTNs.

#### 4.2 Link-targeted attacks

Considering link-targeted attacks we concentrate here on those scenarios that have proven to be most harmful for node-targeted variants, namely removing links with highest degree and highest betweenness centrality. Our aim is to check how resilient the two PTNs are to attacks on links following the corresponding scenarios. However, to proceed we need to generalize the notions of degree and betweenness for the case of links. We define the degree  $k^{(l)}$  of the link between nodes  $i$  and  $j$  with degrees  $k_i$  and  $k_j$  as [13, 20]:

$$k_{ij}^{(l)} = k_i + k_j - 2. \quad (12)$$

With this definition, the link degree is  $k^{(l)} = 0$  for a graph with two vertices and a single link, while for any link in a connected graph with more than two vertices the link degree will be at least one,  $k^{(l)} \geq 1$ . The generalization of betweenness centrality for a link  $e$  is straightforward:

$$\mathcal{C}_B^{(l)}(e) = \sum_{s \neq t \in \mathcal{N}} \frac{\sigma_{st}(e)}{\sigma_{st}}, \quad (13)$$

where  $\sigma_{st}$  is the number of shortest paths between the two nodes  $s, t \in \mathcal{N}$ , that belong to the network  $\mathcal{N}$ , and  $\sigma_{st}(e)$  is the number of shortest paths between nodes  $s$  and  $t$  that go through the link  $e$  (c.f. formula (5) for the node betweenness centrality). By definition,  $\mathcal{C}_B^{(l)}(e)$  measures the importance of a link  $e$  with respect to the connectivity between the nodes of the network.

Fig. 4 shows the results of our simulations for three different attack scenarios, where the PTN links are removed at random (RL) or according to lists ordered by decreasing link degrees and link betweenness centrality. As in the case of node-targeted attacks these lists were recalculated after each step of 1% of link removal. The figure shows the relative size of the largest component of the PTN as function of the share of removed links. Let us first note that the removal of a link does not necessarily lead to a decrease in  $S$ . Indeed, as we see from the figure  $S$  may remain unchanged for small enough values of  $c$ , depending on the attack scenario. This is different from the node-targeted attacks, where the removal of a node decreases the size of  $S$  at least by the relative share of this node. In this respect, the most particular behavior is observed for the highest link degree scenario (red curves in Fig. 4). The value of  $S$  first remains practically unchanged (up to a concentration of removed links  $c \sim 0.08$  for London PTN and even  $c \sim 0.36$  for Paris PTN) and then abruptly decreases almost to zero. This behavior however is an artifact of the recalculated link degree scenario: after removal of the top 1% of links linked to highest degree nodes these nodes may remain connected and will in general

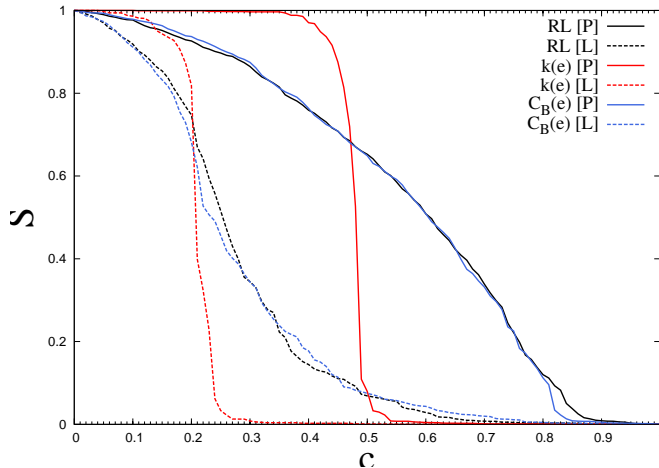


**Fig. 4** Relative size of the largest component of the Paris and London PTNs for different link attack scenarios. RL: random removal of a link,  $k(e)$ ,  $C_B(e)$ : highest link degree and highest link betweenness scenarios. Here, the links (not the nodes) are removed. Hence,  $c$  denotes the share of removed links. As in Fig. 2, a letter in square brackets refer to the London [L] or Paris [P] PTN.

not be targeted in the next step after recalculation. Therefore many steps are needed to strip these nodes off all their links. To further quantify the impact of different scenarios we have calculated the value of the resilience measure  $A$ , introduced in the previous section, see Eq. (8). We present the results for all three scenarios in Table 2. As shown in the table, almost for all link-targeted scenarios the values of  $A$  is almost twice as large for the Paris PTN in comparison with the London PTN. Another obvious observation is that different scenarios applied to the same PTN lead to similar values of  $A$ . Returning back to Fig. 4 it is obvious that not only the resilience measure  $A$  but also the  $S(c)$  curves demonstrate very similar behavior following both random and link betweenness scenarios.

Based on the above simulated attack scenarios we observe that under almost all of these the London PTN appears to be more vulnerable than the Paris PTN. One may therefore ask if there are a-priori criteria that may indicate network resilience prior to any (simulated) attack. In former analysis [13, 20] we found, that a useful criterion for resilience of PTNs with respect to link-targeted attacks is the mean node degree  $\langle k \rangle$  of the unperturbed network. Typically, networks with a higher mean node degree are more resilient. Furthermore, in a recent study on the link-targeted resilience of fourteen different PTNs of major cities [13, 20], the resilience measure  $A$  was found to almost linearly increase with  $\langle k \rangle$ . This appears to indicate that network (link) resilience depends primarily on the initial 'density' of network links, almost independent of possible correlations within the PTN structure. To some extent this is different to the criteria discussed in the former subsection for the node-targeted attacks, where the correlations were considered involving the second moment

of the node degree distribution  $\langle k^2 \rangle$  that enters the Molloy-Reed parameters (9), (11). Comparing  $\langle k \rangle$  for the two unperturbed PTNs (table 1) one can see that its value for Paris PTN exceeds that for London PTN almost in 1.4 times (2.60 for London and 3.73 for Paris, see the table). This observation may be taken as an indicator for a correspondingly higher resilience of the Paris PTN.

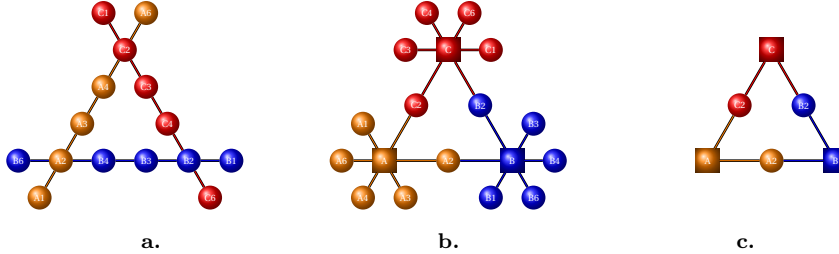


**Fig. 5** a: A graph with three routes, each shown in a separate color; b: the corresponding bipartite graph - route nodes are depicted as square boxes; c: the weeded graph without dangling station nodes.

## 5 One step further: Cascading effects

The approaches to network attack as described in the previous sections assume that any attack on a given station will in first place affect the attacked station and the links to its direct neighbors within the network. The operation of all traffic on the transit network is in this view unaffected on all other links and nodes within the network. This implies some non-realistic situations: e.g. if a subway station X on the London tube ceases to function the model assumes that all routes that would otherwise pass through that station will be split into two halves that continue to function as normal on the remaining parts of that route. Obviously this will in general not happen and instead the route as a whole will cease to operate or at least be seriously reduced in its function.

We therefore embark in this final section to explore the impact of attacks on the network including the cascading effects on all routes that service the attacked station in assuming that all routes that service that station will cease to operate.

This task may be considerably simplified by re-interpreting the network in terms of a so-called bipartite graph. The procedure is illustrated in Fig. 5. Every route is represented by a square vertex connected to the nodes of all its stations, see 5a,b. In a further simplifying step we weed out all stations that are connected to a single route only, as they do not contribute to the connectivity of the network, see 5c.

Within this bipartite network we identify the station node with highest betweenness following the same procedure as above. That node and all adjacent

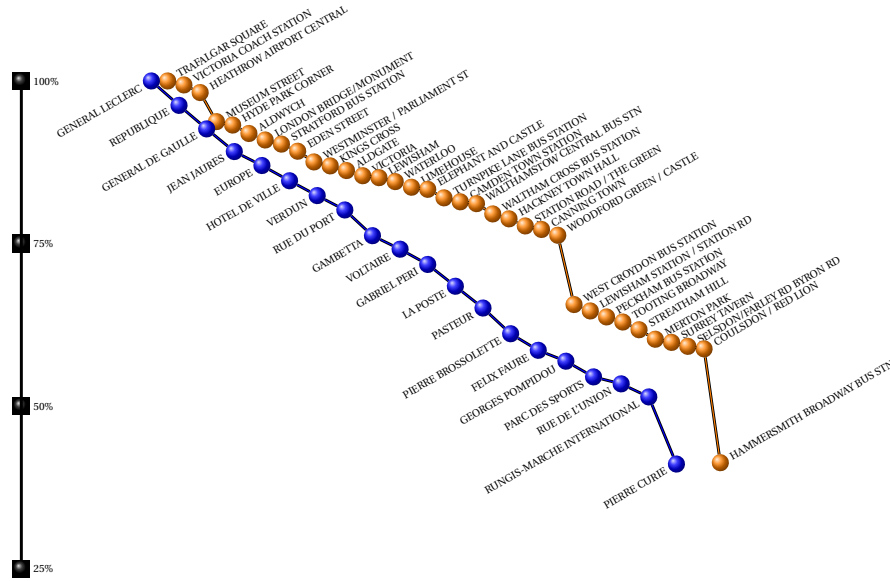


**Fig. 6** The break down of the connected component of the London (light yellow) and Paris (dark blue) PTN under cascading effects, see the text for the attack scenario. For each step of the attack we depict the corresponding station with highest betweenness that is subsequently removed. The axis on the left indicates the remaining percentage of the connected part of the network.

routes are then removed - as will all station nodes that become disconnected in this process.

The latter step is repeated until the largest connected component in the remaining network is smaller than half of the original bipartite graph indicating complete breakdown of the network.

Following this procedure we find that both the Paris and the London network reach the 50% breakdown point when only 0.47% of the total stations become dysfunctional. This corresponds to 34 stations of the London PTN and 19 stations of the Paris network. Fig. 6 depicts the break down of the connected component of the network. For each step of the procedure we depict the corresponding station with highest betweenness that is subsequently removed. The axis on the left indicates the remaining percentage of the connected part of the network. We close by noting that on an operational basis the network may break down even much earlier, than predicted by our theory as far as the load to be transferred to the remaining routes will far exceed by far the capacity of these at an even lower number of dysfunctional routes.

**Acknowledgements** We thank Ralph Kenna for helpful discussions and a suggestion for the title. This work was supported by FP7 grant SPIDER (Statistical Physics in Diverse Realisations) PIRSES-GA-2011-295302.

## References

1. R. Albert, A.-L. Barabási, *Rev. Mod. Phys.* **74**, 47 (2002); S. N. Dorogovtsev, J. F. F. Mendes, *Adv. Phys.* **51**, 1079 (2002); M. E. J. Newman, *SIAM Review* **45**, 167 (2003).
2. D. J. Watts, *Small Worlds*. Princeton University Press, Princeton, NJ (1999); S. N. Dorogovtsev, S. N. Mendes, *Evolution of Networks*. Oxford University Press, Oxford (2003); M. E. J. Newman, A.-L. Barabási, D. J. Watts, *The Structure and Dynamics of Networks*. Princeton University Press, Princeton (2006).
3. D. Stauffer, A. Aharony, *Introduction to Percolation Theory*. Taylor & Francis, London (1991).
4. S. Bornholdt, H. Schuster (Eds.), *Handbook of Graphs and Networks*. Wiley-VCH, Weinheim (2003).
5. B. Bollobás, *Random Graphs*. Academic, London (1985).
6. M. Marchiori, V. Latora, *Physica A* **285**, 539 (2000); V. Latora, M. Marchiori, *Phys. Rev. Lett.* **87**, 198701 (2001); V. Latora, M. Marchiori, *Physica A* **314**, 109 (2002).
7. K. A. Seaton, L. M. Hackett, *Physica A* **339**, 635 (2004).
8. P. Angeloudis, D. Fisk, *Physica A* **367**, 553 (2006); S. Derrible, C. Kennedy, *Transportation* **37**, 275 (2010); S. Derrible, C. Kennedy, *Physica A* **389**, 3678 (2010).
9. J. Sienkiewicz, J. A. Holyst, *Phys. Rev. E* **72**, 046127 (2005); J. Sienkiewicz, J. A. Holyst, *Acta Phys. Polonica B* **36**, 1771 (2005).
10. P.-P. Zhang, K. Chen, Y. He, T. Zhou, B.-B. Su, Y. Jin, H. Chang, Y.-P. Zhou, L.-C. Sun, B.-H. Wang, D.-R. He, *Physica A* **360**, 599 (2006); X. Xu, J. Hu, F. Liu, L. Liu, *Physica A* **374**, 441 (2007); H. Chang, B.-B. Su, Y.-P. Zhou, D.-R. He, *Physica A* **383**, 687 (2007); Z.-T. Zhu, J. Zhou, P. Li, X.-G. Chen, *Chinese Physics B* **17**, 2874 (2008).
11. C. von Ferber, Yu. Holovatch, V. Palchykov, *Condens. Matter Phys.* **8**, 225 (2005); C. von Ferber, T. Holovatch, Yu. Holovatch, V. Palchykov, *Physica A* **380**, 585 (2007); C. von Ferber, T. Holovatch, Yu. Holovatch, V. Palchykov, *Eur. Phys. J. B* **68**, 261 (2009).
12. S. Derrible, C. Kennedy, *Transport Reviews* 1-25 (2011).
13. T. Holovatch, *Complex Transportation Networks: Resilience, Modelling and Optimisation*, Ph.D. thesis, Nancy University, France & University of Coventry, GB (2011). <http://tel.archives-ouvertes.fr/tel-00652784/fr/>
14. P. Holme, B. J. Kim, C. N. Yoon, S. K. Han, *Phys. Rev. E* **65**, 056109 (2002).
15. B. Berche, C. von Ferber, T. Holovatch, Yu. Holovatch, *Eur. Phys. J. B* **71**, 125 (2009); B. Berche, C. von Ferber, T. Holovatch, Yu. Holovatch, *Dynamics of Socio-Economic Systems* **2**, 42 (2010).
16. U. Brandes, *J. Math. Sociology*, **25**, 163 (2001).
17. R. Cohen, S. Havlin, D. ben-Avraham, *Phys. Rev. Lett.* **91**, 247901 (2003).
18. M. Girvan, M. E. J. Newman, *Proc. Natl. Acad. Sci. USA* **99**, 7821 (2002).
19. C. M. Schneider, T. Mihaljev, S. Havlin, H. J. Herrmann, *Phys. Rev. E* **84** 061911 (2011); C. M. Schneider, A. A. Moreira, J. S. Andrade, Jr., S. Havlin, H. J. Herrmann, *Proc. Natl. Acad. Sci. USA* **108**, 3838 (2011).
20. B. Berche, C. von Ferber, T. Holovatch, Yu. Holovatch. *Advances in Complex Systems* **15** 1250063 (2012); preprint arXiv:1201.5532v1 (2012).
21. M. Molloy, B. A. Reed, *Random Struct. Algorithms* **6(2/3)**, 161 (1995); M. Molloy, B. Reed, *Combinatorics, Probability and Computing* **7**, 295 (1998)
22. R. Cohen, K. Erez, D. ben-Avraham, S. Havlin, *Phys. Rev. Lett.* **85**, 4626 (2000) D. S. Callaway, M. E. J. Newman, S. H. Strogatz, D. J. Watts, *Phys. Rev. Lett.* **85**, 5468 (2000).